

# Analysis of Magneto-Rheological (MR) Damper and its Application in Vehicle Suspension System

Wasim Ruskin Khan

Mechanical School of Engineering Lovely Professional University  
E-mail: [ruskinkhan40@gmail.com](mailto:ruskinkhan40@gmail.com)

**Abstract**—To control vibration, magneto-rheological (MR) damper is one of the best semi-active dampers. One of the reasons for its increasing use in vehicle suspension system is its controllability in both on-state and off-state damping forces. But there are some parameters that need to be improved like MR fluid's sedimentation, geometry design optimization, use of materials. This research aims at developing and enhancing the performance of an MR damper system facility by means of simulation by ANSYS 15 and algebraic equations in order to accommodate various input loads. The development of the suspension system began with a comprehensive research in this particular field so as to identify various areas for improvement. The aim of this research is to increase the on-state damping forces of a standard model of an MR damper by altering different geometric parameters, changing material properties and materials. Different models are identified and analyzed to improve the on-state damping force. The study revealed two cases, first is high on-state force at low current and second, overall maximum on-state force.

## 1. INTRODUCTION

Magneto-rheological (MR) fluids are smart materials which respond to an applied magnetic field. MR fluid is composed of micro-sized magnetic particles such as carbonyl iron particles suspended in an insulating carrier liquid like hydrocarbon oil, silicon oil, glycol etc. [1, 2]. The suspended particles become magnetized and align themselves in chain like structure in the direction of the magnetic field as shown in figure 1.1. These chains restrict the movement of the MR fluid and thereby increase theyield stress of the fluid. In the “off” state, the MR fluids appear similar to liquid paints and exhibit comparable levels of apparent viscosity (0.1 to 1 Pa-s at low shear rates) [3]. Their apparent viscosity changes dramatically (105-106 times) within a few milliseconds when the magnetic field is applied. The change in the viscosity of the MR fluid is completely reversible when the magnetic field is removed [4].

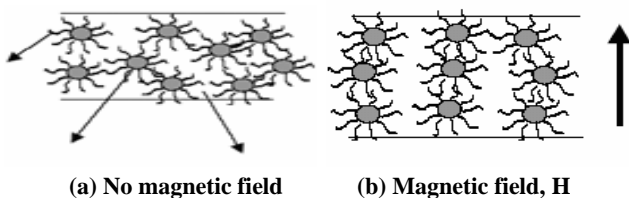


Fig. 1.1: Chain-like formation of Magnetic particles in MR fluids in the direction of an applied magnetic field [4]

## 1.1 Why MR fluid?

MR fluids have recently become a smart fluid because of its versatile characteristics. Another class of fluids that exhibit a rheological change is electro-rheological (ER) fluids which exhibit rheological changes when an electric field is applied to the fluid. However, there are some drawbacks in ER fluid such as it is vulnerable to change in temperature viz. extreme property changes with temperature and also relatively small rheological changes to MR fluid [5].

The MR fluid allows one to control the damping force of the damper by replacing mechanical valves commonly used in adjustable dampers. This has the potential for a superior damper with lesser concern about reliability because if the MR damper ceases to be controllable then it simply acts as a passive damper.

## 1.2 MR damper

The design of vehicle suspension is one of the important factors in the dynamics of a vehicle which has to satisfy the demanding requirements in providing good ride comfort, vehicle handling and stability. There are broadly three types of vehicle suspensions - passive, semi-active and active suspensions. The commonly used passive suspension having an oil damper provides design simplicity and cost-effectiveness in practical application but due to lack of damping force controllability, its performance is limited. The active suspension however, having separate actuators that can exert an independent force provides high control performance in a wide frequency range but the cost and complexity of the system limits its commercial applications. To solve these issues, researches on vibration control using semi-active suspensions have significantly increased since semi-active suspensions can provide performance benefits over passive suspensions and without requiring large power sources and expensive hardware like active suspensions. Recently, MR dampers as semi-active suspension systems are being used in a large number of vehicles which can satisfy the conflicting demands in a wide range [6, 7]. Researchers and engineers have interests in MR damper because of its flexible damping

character, mechanical simplicity, less power consumption, quick response and compliance with electronic control [8].

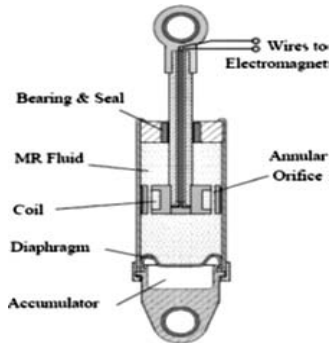


Fig. 1.2: RD-1005-3 MR damper manufactured by Lord Corporation [9, 10]

2. METHODOLOGY

In this work, the piston head of a standard model of an MR damper is analyzed by finite element methods using ANSYS 15 [11]. Design of some of the parameters in MR dampers are modified that can have a significant effect on the on-state force-current relationship of MR dampers. The effects of different geometric designs, material properties and materials on increasing the damping force that can result from an MR damper with a given size are evaluated by simulation and algebraic expressions.

2.1 Mathematical formulations

The on-state damper force of the MR damper, **F** can be expressed as [12];

$$F = \Delta P_{\tau} A_{\tau}; \text{ where,}$$

$\Delta P_{\tau}$  = On state pressure component or field dependent induced yield pressure component

$A_{\tau}$  = Active fluid area

The field stress component  $\Delta P_{\tau}$  and active fluid area  $A_{\tau}$  can be written as;

$$\Delta P_{\tau} = \frac{c\tau_y L}{g}$$

$$A_{\tau} = 2\pi b(L+g); \text{ where,}$$

c= Constant (c=3, in this case)

$\tau_y$  = Field dependent yield stress

or fluid shear stress

L= Length of fluid flow orifice

g= Fluid gap (annular gap)

a= Inner radius of the engine

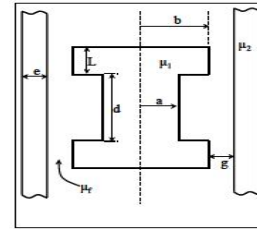


Fig. 2.1: Schematic representation of piston head, housing and fluid gap

b= Outer radius of the engine

d= Length of spool

e= Thickness of housing

$\mu_1, \mu_2, \mu_f$  = Permeability of engine, housing and MR fluid respectively

Now, the fluid shear stress ( $\tau_y$ ) can be expressed as a function of magnetic flux density or magnetic induction (B) as[13];

$$\tau_y = 6.298B^4 - 25.824B^3 + 26.639B^2 - 0.438B$$

The magnetic flux density(B) in the above equation is analyzed by using ANSYS 15.

3. RESULTS AND ANALYSIS

Model 1. Standard model

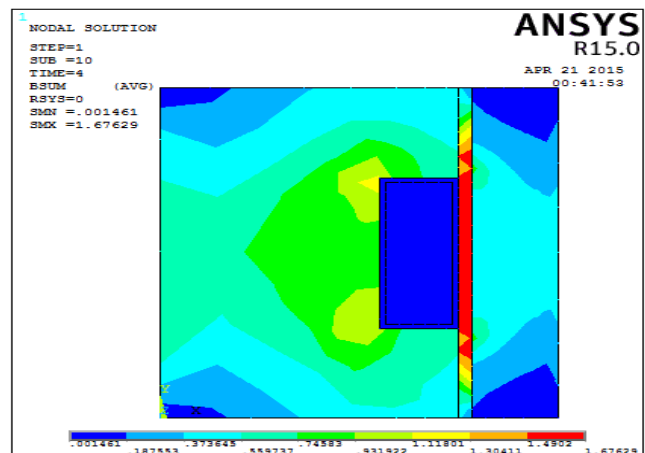
Material properties

Relative permeability of engine and housing=80 (Martensitic stainless steel)

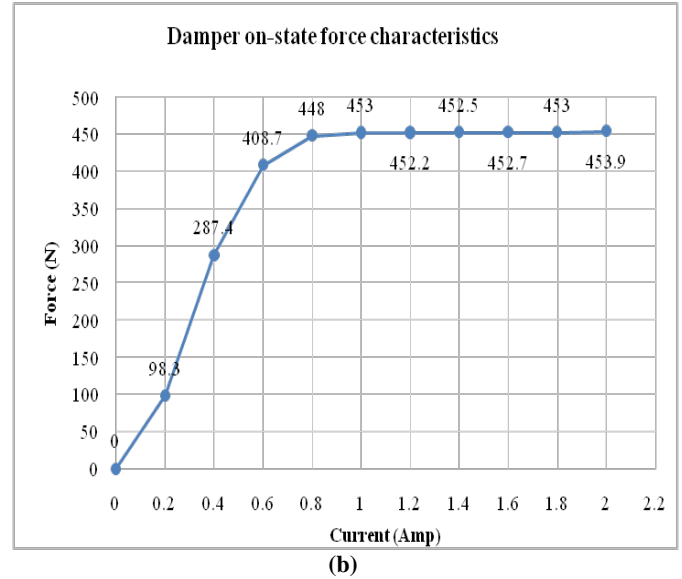
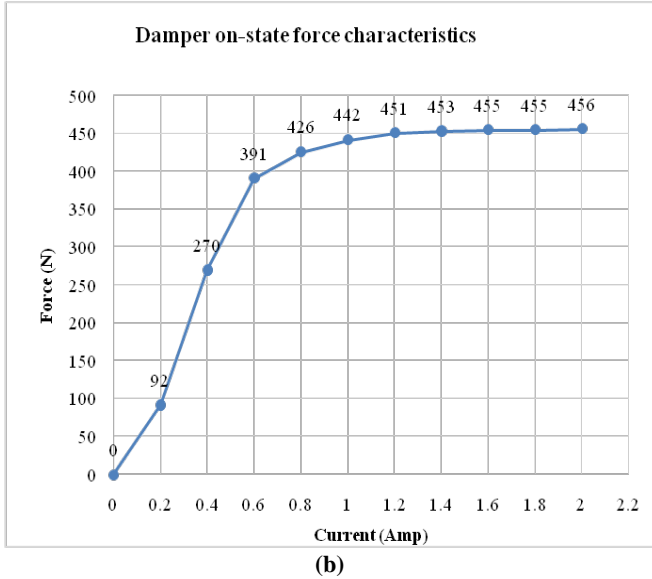
MR fluid particles= silicon cored iron

Relative permeability of coil=0.99(copper)

Relative permeability of air gap=1 (air)



(a)



Maximum On-state force=456 N  
Current=2.0 Amp

Average  $B_{sum} = 0.84$  T

Fig. 3.1: (a) ANSYS model at max. on-state force  
(b) On-state Forces vs. Current graph

Maximum On-state force=453.9 N  
Current=2.0 Amp

Average  $B_{sum} = 0.834$  T

Fig. 3.2: (a) ANSYS model at max. Force  
(b) Graph between On-state Forces vs. Current

**Model 2. Chamfered ends (Chamfered from each corner of the MR fluid gap=1mm)**

Material properties

Relative permeability of engine and housing=80  
(Martensitic Stainless steel)

MR fluid particles= Silicon cored iron

Relative permeability of coil=0.99(Copper)

Relative permeability of air gap=1(air)

**Model 3. Fluid gap increased by 0.5 mm and housing area reduced by 0.5mm (A)**

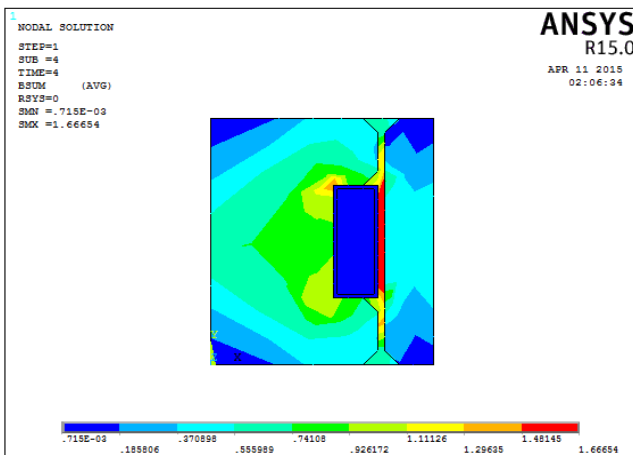
Material properties

Relative permeability of engine and housing=80 (Martensitic stainless steel)

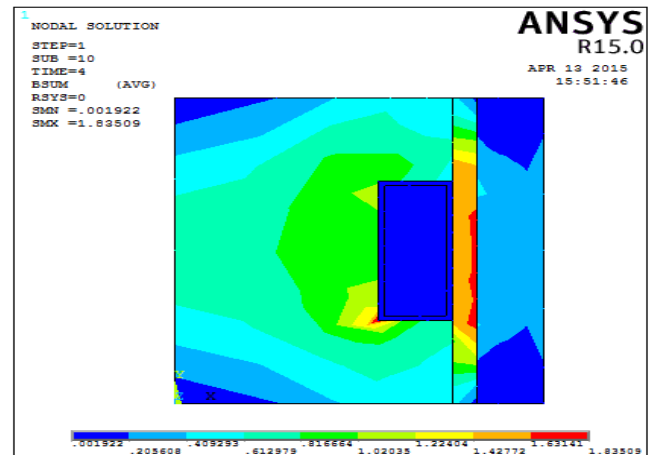
MR fluid particles= Silicon cored iron

Relative permeability of coil=0.99(Copper)

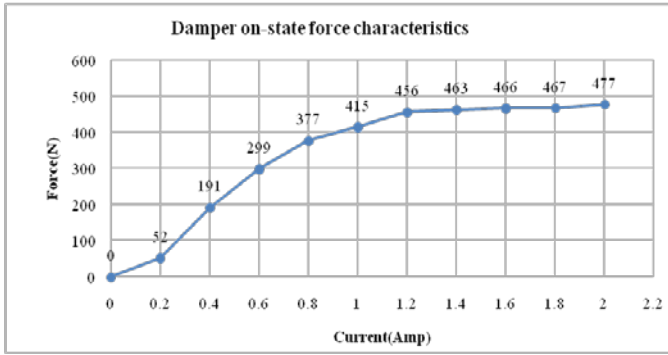
Relative permeability of air gap=1(air)



(a)



(a)



(b)

Maximum On-state force= 477 N

Current=2.0 Amp

Average  $B_{sum} = 0.918$  T

Fig. 3.3: (a) ANSYS model at max. on-state force  
(b) On-state Forces vs. Current graph

**Model 4. Fillet Ends A (Fillet radius=1.5mm)**

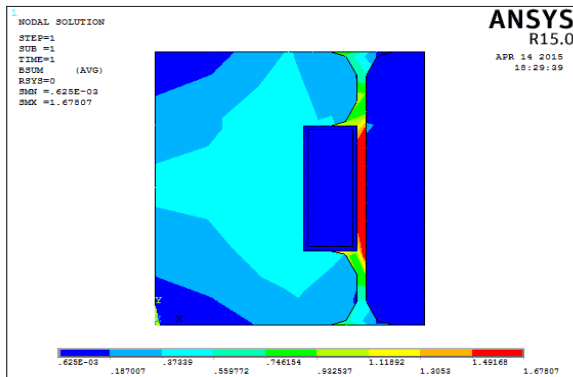
Material properties

Relative permeability of engine and housing= 80 (Martensitic stainless steel)

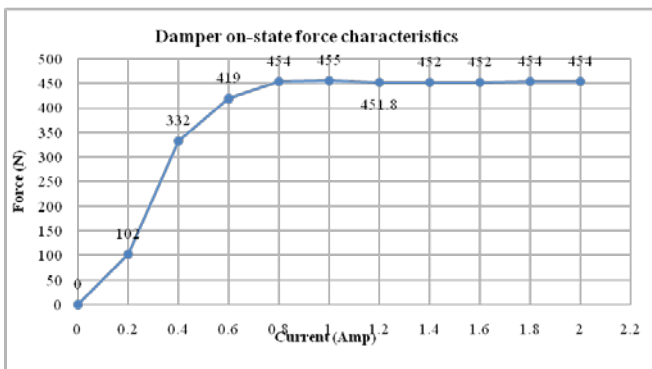
MR fluid particles= Silicon cored iron

Relative permeability of coil=0.99(Copper)

Relative permeability of air gap=1(air)



(a)



(b)

Maximum On-state force= 455 N

Current=1.0 Amp

Average  $B_{sum} = 0.84$  T

Fig. 3.4: (a) ANSYS model at max. on-state force  
(b) On-state Forces vs. Current graph

**Model 5. Fillet Ends B (Fillet radius=1.5mm)**

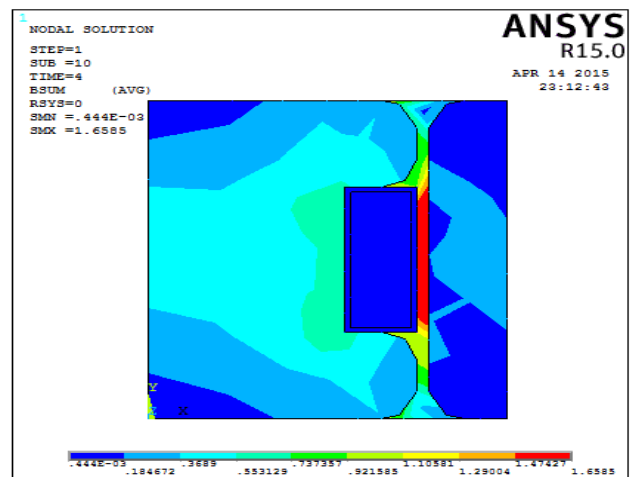
Material properties

Relative permeability of engine and housing= 45 (Martensitic stainless steel)

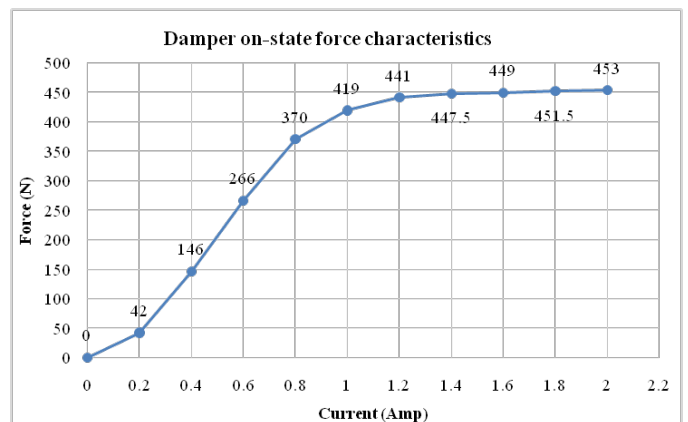
MR fluid particles= Silicon cored iron

Relative permeability of coil=0.99(Copper)

Relative permeability of air gap=1 (air)



(a)



(b)

Maximum On-state force= 453 N

Current=2.0 Amp

Average  $B_{sum} = 0.829$  T

Fig. 3.5: (a) ANSYS model at max. on-state force  
(b) On-state Forces vs. Current graph

**Model 6. Fillet Ends C(Fillet radius=1.5mm)**

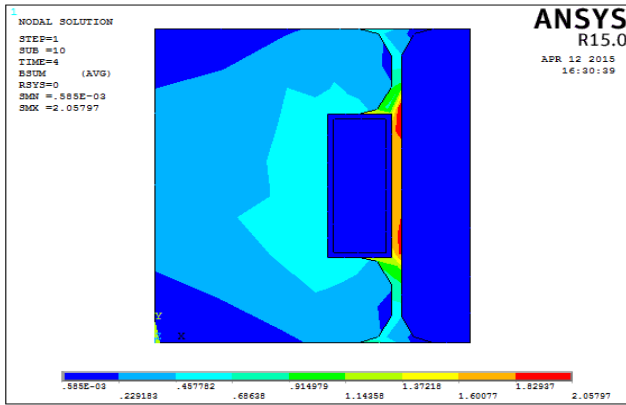
Material properties

Relative permeability of engine and housing=80 (Martensitic stainless steel)

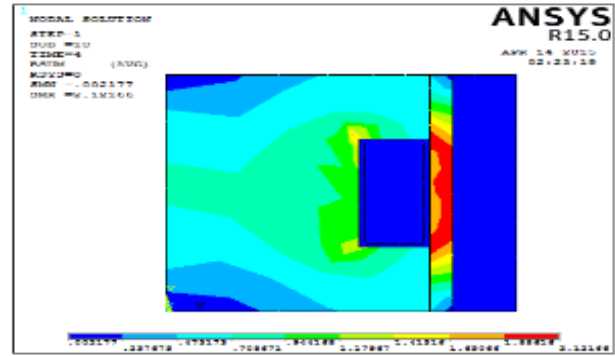
MR fluid particles= Ferro Cobalt: 34.5% Co

Relative permeability of coil=0.99(copper)

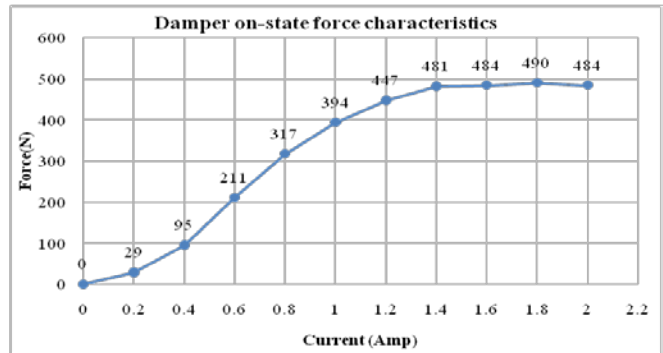
Relative permeability of air gap=1(air)



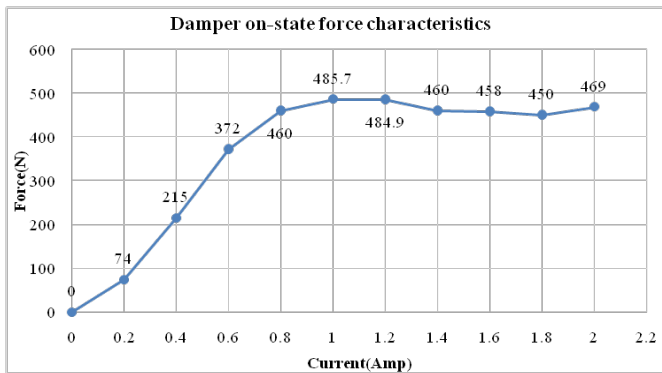
(a)



(a)



(b)



(b)

Maximum On-state force= 485.7 N

Current=1.0 Amp

Average  $B_{sum}$  =1.03 T

**Fig. 3.6: (a) ANSYS model at max. on-state force (b) On-state Forces vs. Current graph**

**Model 7. Fluid gap increased by 0.5 mm and housing area reduced by 0.5mm (B)**

Material properties

Relative permeability of engine and housing=80 (Martensitic stainless steel)

MR fluid particles= Ferro Cobalt: 34.5% Co

Relative permeability of coil=0.99(copper)

Relative permeability of air gap=1(air)

Maximum On-state force= 490 N

Current=1.8 Amp

Average  $B_{sum}$  =1.06 T

**Fig. 3.7: (a) ANSYS model at max. on-state force (b) On-state Forces vs. Current graph**

**Model 8. Fillet ends and fluid gap increased by 0.5 mm and housing area reduced by 0.5mm (Fillet radius=1.5mm)**

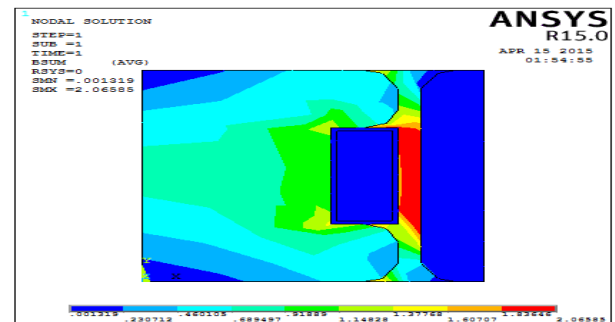
Material properties

Relative permeability of engine and housing=80 (Martensitic stainless steel)

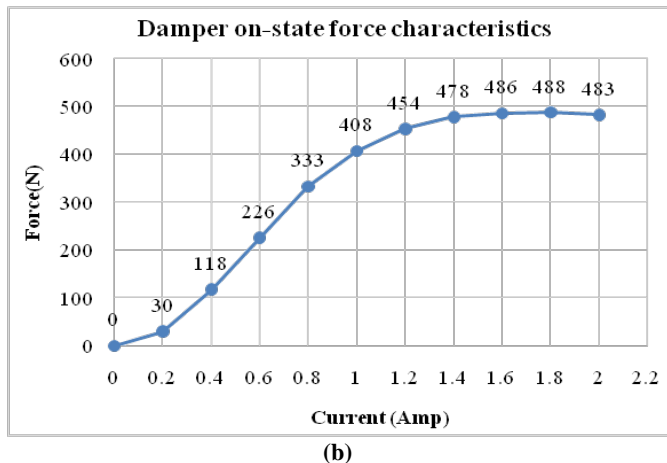
MR fluid particles= Ferro Cobalt: 34.5% Co

Relative permeability of coil=0.99(copper)

Relative permeability of air gap=1(air)



(a)



(b)

Maximum On-state force= 488 N

Current=1.8 Amp

Average  $B_{sum} = 1.033$  T

**Fig. 3.8: (a) ANSYS model at max. on-state force  
(b) On-state Forces vs. Current graph**

From the above analysis, it is clear that Model 6 generates maximum force at least current. The changes in Model 6 from Model 1 (standard model) are in geometry as well as in the materials used. The fillet ends and the use of Ferro Cobalt: 34.5% Co as magnetic fluid particles in Model 6 give rise to an on-state force of 485.7 N in 1 Amp compare to 442 N in 1 Amp in Model 1. However, if minimization of current is not a factor and the requirement of maximum force is concerned only, then Model 7 is the most optimized model for this case. This model generates maximum on-state force of 490 N at 1.8 Amp compare to maximum on-state force of 456 N at 2 Amp in Model 1. If the properties of Model 6 and Model 7 are merged, the resultant Model 8 doesn't show any optimal value. Hence for a maximum force at low current and for an overall maximum force Model 6 and Model 7 respectively are the most optimized models.

#### 4. CONCLUSION

One of the most important parameters in designing MR dampers is to obtain maximum force at minimum space. In order to identify the best geometrical configuration, several configurations of the MR damper are studied to ascertain how altering different parameters affects the on-state damper force. The best configurations which give the maximum on-state force as output are considered.

A finite element analysis (FEA) model for 2D axisymmetric model of MR damper's engine, coil, air gap, MR fluid gap and housing is obtained. For a 2-D axisymmetric model of an MR damper, different geometric parameters, materials and material properties that affect the magnetic field and on-state force of the damper are studied and the relationship between on-state force and current is obtained. After simulating and

analyzing different models it can be concluded that, Model 6 provides the maximum on-state force at least current and Model 7 provides the overall maximum on-state force at a current of 1.8 Amp. Model 7 can be used in applications where a large on-state force is required and current minimization is not a factor.

#### REFERENCES

- [1] Shuqi Guo, Zhigang Xia, Shaopu Yang, "Nonlinear vibrations of vehicle suspension systems with magnetorheological dampers," Vehicular Electronics and Safety, IEEE International Conference, DOI: 10.1109/ICVES.2005.1563664.
- [2] Guo, D., and Hu, H., 2005, "Nonlinear Stiffness of a Magneto-Rheological Damper," *Nonlinear Dyn.*, **40**(3), pp. 241–249.
- [3] Kordonsky W O, Ashour, Rogers C A. Magneto rheological fluids: materials, characterization, and devices [J]. *Journal of Intelligent Material Systems and Structures*, 1996(7):123-130.
- [4] Muhammad Aslam, Yao Xiong-liang, and Deng Zhong-chao, "Review of magnetorheological (MR) fluids and its applications in vibration control" *Journal of Marine Science and Application*, Vol.5, No.3, September 2006, pp. 17-29.
- [5] Jolly, M. R., J. W. Bender, and J. D. Carlson. 1999. "Properties and Applications of Commercial Magnetorheological Fluids." *Journal of Intelligent Material Systems and Structures* 10(1):5–13.
- [6] L. Balamurugan, J. Jancirani and M. A. Eltantawie, "Generalized Magneto- Rheological (MR) Damper Model and Its Application in Semi-Active Control Of Vehicle Suspension System," *International Journal of Automotive Technology*, Vol. 15, No. 3, pp. 419–427 (2014).
- [7] S. Sigla and S. Reich, technical university of Kosice, Slovakia, "Optimization and Characterization of passive, active and semi-active vehicle suspension systems." 12<sup>th</sup> IFToMM World Congress, Besancon (France), June 18-21, 2007.
- [8] Parlak, Z., Engin, T., and Çallı, İ., 2012, "Optimal design of MR damper via finite element analyses of fluid dynamic and magnetic field," *Mechatronics*, **22**(6), pp. 890–903.
- [9] XIANG Hengbo, FANG Qin, GONG Ziming, WU Hao, 2008, "Experimental Investigation into Magnetorheological Damper Subjected to Impact Loads\*," *Trans. Tianjin Univ.* 2008, 14:540-544.
- [10] Bica, Ioan, Ying Dan Liu, and Hyoung Jin Choi. 2013. "Physical Characteristics of Magnetorheological Suspensions and Their Applications." *Journal of Industrial and Engineering Chemistry* 19 (2):394–406.
- [11] Ferdous, M. M., Rashid, M. M., Hasan, M. H., and Rahman, M. A., 2014, "Optimal design of Magneto-Rheological damper comparing different configurations by finite element analysis †," **28**(9), pp. 3667–3677.
- [12] Salloom, M. Y., and Samad, Z., 2011, "Finite element modeling and simulation of proposed design magneto-rheological valve," pp. 421–429.
- [13] W. H. El-Aouar, M. Ahmadian, D. J. Inman, D. Leo, 2002, "Finite Element based modelling of Magneto Rheological Dampers," pp. 3-13, pp103-104.